PHYSICAL REVIEW B **96**, 100504(R) (2017)

Anomalous temperature evolution of the electronic structure of FeSe

Y. S. Kushnirenko,[1,*] A. A. Kordyuk,[2,3] A. V. Fedorov,[1,4] E. Haubold,[1] T. Wolf,[5] B. Büchner,[1] and S. V. Borisenko[1]

[1]*IFW Dresden, Helmholtzstrasse 20, 01069 Dresden, Germany*

[2]*Institute of Metal Physics of National Academy of Sciences of Ukraine, 03142 Kyiv, Ukraine*

[3]*Kyiv Academic University, 03142 Kyiv, Ukraine*

[4]*II. Physikalisches Institut, Universität zu Köln, Zülpicher Strasse 77, 50937 Köln, Germany*

[5]*Institute for Solid State Physics, Karlsruhe Institute of Technology, 76131 Karlsruhe, Germany*

(Received 7 February 2017; revised manuscript received 7 August 2017; published 15 September 2017)

We present angle-resolved photoemission spectroscopy data taken from the structurally simplest representative of iron-based superconductors, FeSe, in a wide temperature range. Apart from the variations related to the nematic transition, we detect very pronounced shifts of the dispersions on the scale of hundreds of degrees Kelvin. Remarkably, upon warming up the sample, the band structure has a tendency to relax to the one predicted by conventional band structure calculations, directly opposite to what is intuitively expected. Our findings shed light on the origin of the dominant interaction shaping the electronic states responsible for high-temperature superconductivity in iron-based materials.

DOI: 10.1103/PhysRevB.96.100504

Iron-based superconductors (IBSs) continue to represent another class of materials with an unknown mechanism of pairing at high temperatures. The electronic structure of iron pnictides and chalcogenides has two essential deviations from the predictions of conventional band structure calculations, and these deviations may hold the key to understanding the phenomenon. The first pronounced departure from local density approximation (LDA) calculations is the strong renormalization of the valence band with orbital-dependent factors ranging from 2 to 9 [1–4]. This behavior has been successfully explained in the framework of dynamical mean-field theory (DMFT) calculations by considering the significant exchange interaction J [5–7]. The second robust, and generic for all IBS families, experimental fact is the so-called "blue/redshifts" which result in mutually opposite energy shifts of the dispersions near the center and the corner of the Brillouin zone (BZ) [2,8–10]. Such shifts lead, in particular, to the shrinking of the Fermi surfaces (FSs) in comparison with the calculated ones and bring the van Hove singularities closer to the Fermi level [11]. There are several theoretical approaches to explain such shifts [12–19], but neither a consensus nor a quantitative agreement with the experiment has been reached.

In this Rapid Communication, we report an unusual temperature dependence of the low-energy electronic structure in FeSe. The energy location of the electronic dispersions clearly changes with temperature and these variations are momentum dependent. The blue/redshifts tend to disappear with temperature and Fermi surfaces grow in size, thus bringing the electronic structure closer to the calculated one. We consider several scenarios which can explain the observed anomaly.

Angle-resolved photoemission spectroscopy (ARPES) data have been collected at the I05 beamline of Diamond Light Source [20]. Single-crystal samples were cleaved *in situ* in a vacuum better than 210–10 mbars and measured at temperatures ranging from 5.7 to 270 K. Measurements were performed using linearly polarized synchrotron light, utilizing a Scienta R4000 hemispherical electron energy analyzer with an angular resolution of 0.2–0.5 and an energy resolution of 3 meV. Samples were grown by the $KCl/AlCl_3$ chemical vapor transport method.

We start presenting the ARPES data by showing a typical Fermi surface map of FeSe in Fig. 1(a). There are several sheets: one that is holelike, located in the center of the BZ, and two electronlike, located at the corners. The shape of all FSs is modified by the electronic nematicity below 90 K and by the presence of the domains [2,9,17,21–28]. The circular pocket at the center in the tetragonal phase [shown schematically in Fig. 1(a)] is replaced by two slightly elliptical pockets from different domains and the crossed ellipses in the corners are more elongated [29]. As has been pointed out in previous ARPES reports, the experimental Fermi surfaces are noticeably smaller than those obtained by the band structure calculations [1,2,9,21–28]. Figure 1(b) clarifies why this is the case. It shows the experimental dispersions along the diagonal direction of the BZ running through both discussed regions of the k space. It is seen that both hole- and electronlike bands have their extrema close to the Fermi level, and this makes the corresponding Fermi surfaces small.

We have recorded the temperature evolution of these two main constructs from 6 to 270 K. The results are shown in Fig. 2. It is important to distinguish the modifications due to a nematic transition occurring at 90 K from global temperature-induced changes on a larger temperature scale. As was shown earlier [2], orthorhombicity causes an inequality of the dispersions along the ΓX and ΓY directions and results in a small splitting of the features in the ARPES data collected from overlapping domains. The splitting starts to occur at around 90 K and reaches its maximum relatively quickly, in a manner typical for an order parameter. We do not focus on the details of this effect here and concentrate instead on another trend, also clearly seen from the spectra. A visual inspection of Fig. 2 already clearly implies the monotonic shifts of the features with temperature: Electronlike dispersions from the corner of the BZ in the upper row of panels move downward to higher binding energies while the holelike dispersions in the lower row move upward.

*y.kushnirenko@ifw-dresden.de

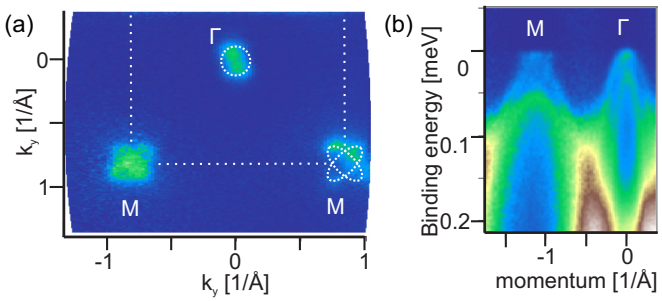

FIG. 1. (a) ARPES-derived Fermi surface map of FeSe. Dashed lines schematically show the shapes of the pockets in the tetragonal phase and boundaries of the BZ. (b) ARPES intensity along the diagonal of the BZ (Γ-*M* direction).

A further detailed quantification of this temperature evolution is presented in Fig. 3. Here, we show intensity plots for single energy distribution curves (EDCs) divided by the Fermi function from the center and the corner of the BZ in the selected temperature intervals [Figs. 3(a) and 3(b)]. Both plots confirm the previously detected trend in Fig. 2. The measure of the temperature-induced shifts can be derived by comparing pairs of EDCs taken at low and high temperatures [Figs. 3(c) and 3(d)]. The difference between the blue and red arrows in Fig. 3(c) is 9.5 meV, and it is 24 meV in Fig. 3(d), i.e., well beyond the experimental errors. We plot the positions of the maximum of the EDC from the center of the BZ (black symbols) in the full studied range of temperatures in Fig. 3(e). As Fig. 3(a) implies, it is even possible to track the maximum of the holelike band which crosses the Fermi level (blue symbols) in a limited temperature interval. This peak can be directly seen in the red EDC in Fig. 3(d) at an approximately −20 meV binding energy. From Fig. 3(e) it is seen that both bands are sensitive to temperature, but below the nematic transition they appear to shift with different speeds. This happens because of an additional splitting between these two bands caused by nematicity [2].

The bottoms of the electron bands [Fig. 3(d)] are situated lower in energy than the tops of the hole bands [Fig. 3(c)], and because of the stronger scattering they are not clearly separated in the EDC's line shape [2,27]. In order to avoid a complicated fitting of the EDCs which usually requires many parameters because of energy-dependent self-energy, we approximate their temperature dependence by tracking the position of the maximum of a single broad feature above the nematic transition [Fig. 3(f)] (for details, see the Supplemental Material [30]) and by the mean value of the binding energies of all four peaks at 6 K. A sketch of the actual temperature evolution of the band structure based on our previous experimental results [2] is shown in Fig. 3(f) with pink dashed lines. There (Fig. 2(g) and Figs. 3(d) and 3(f) in Ref. [2]), we demonstrated that the EDC in the *M* point consists of two features in a tetragonal state and four features in an orthorhombic state.

Obviously, such significant variations in energy of the bands should result in changes of the sizes of the Fermi surfaces. A direct comparison of the Fermi surface maps in Figs. 4(a)–4(d) is in line with all previous statements and seems to be in agreement with the enlargement of both Fermi surfaces upon warming up the sample. We note that in the case of a holelike Fermi surface, which appears larger on the map, one should be careful when analyzing its size quantitatively. The distance between the peaks of the E_F momentum distribution curve (MDC) usually used for this procedure can be inconclusive because at high temperatures this line shape is influenced by two additional factors: The distance between such peaks becomes comparable to their width and the top of another holelike band approaches the Fermi level, and its spectral

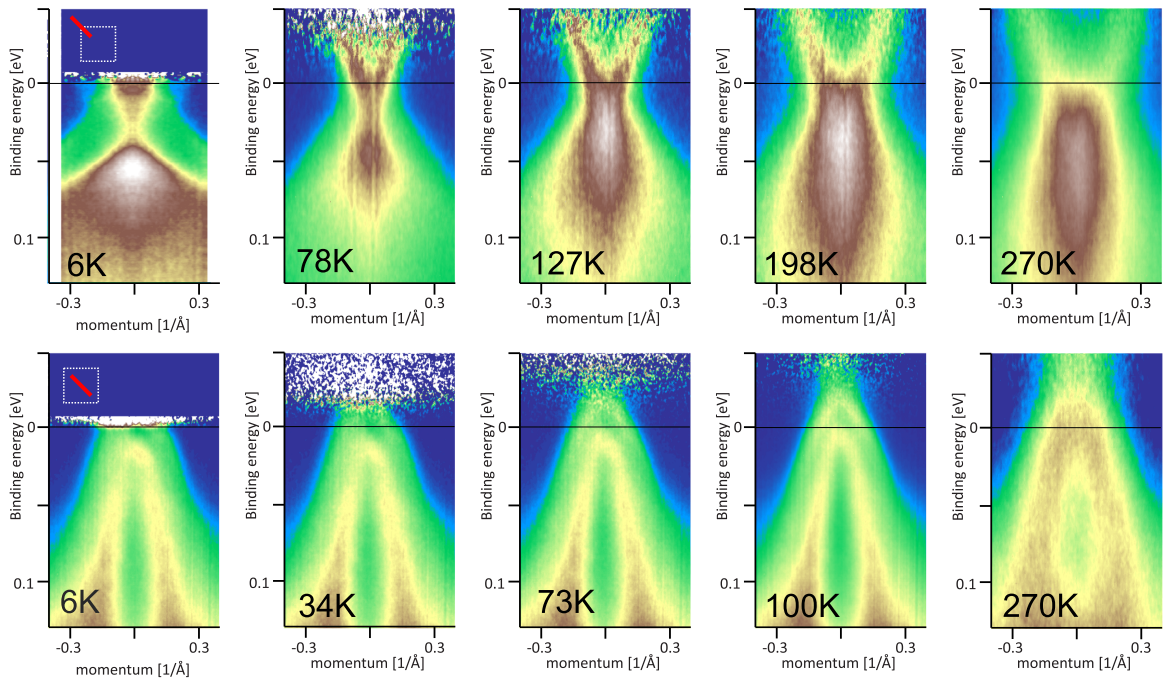

FIG. 2. ARPES intensity plots taken at different temperatures from 6 to 270 K along the diagonal direction through the corner (upper panels) and the center (bottom panels) of the BZ.

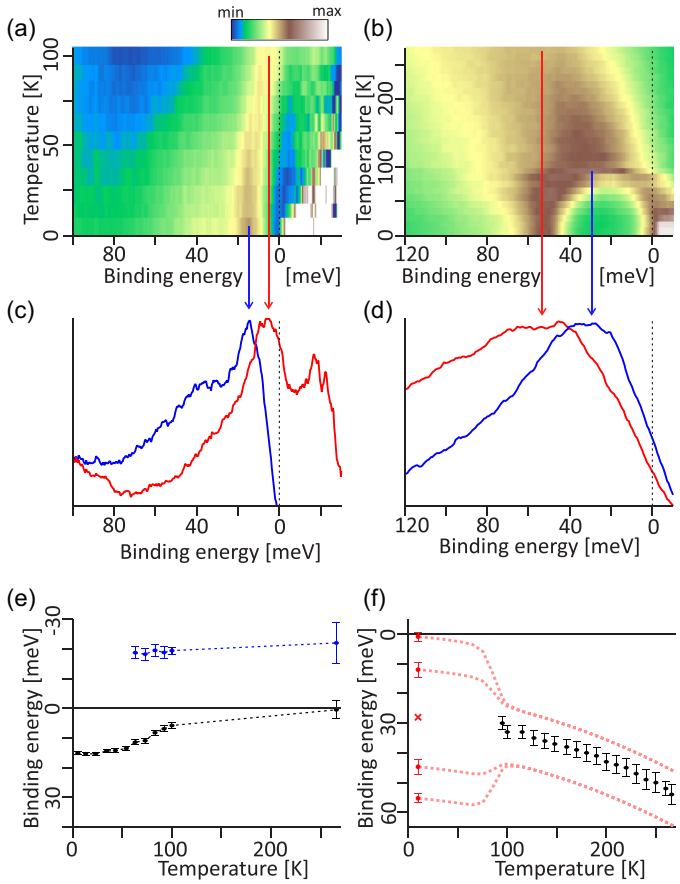

FIG. 3. (a) Intensity plots for single EDCs from the center of the BZ as a function of temperature. All EDCs are divided by the Fermi function. (b) The same for EDCs from the corner of the BZ. (c), (d) Comparison pairs of EDCs with the highest and the lowest temperatures from (a) and (b), respectively. (e) Position of maxima of EDCs from (a) (black dots), which represents the top of the lower and higher hole bands (black and blue dots, respectively). (f) Position of two maxima of EDCs from (b), position of four peaks extracted from EDC measured for 6 K (red dots), and their mean value (red cross). A sketch of the temperature evolution of the band structure is based on our experimental results (pink lines).

weight modifies the E_F MDC. Actually, both these factors visually reduce the size of the hole pocket in Fig. 4(d). For this reason, we will choose different measures to quantify the observed temperature variations in the following.

We schematically summarize the changes observed in this study in Figs. 4(e) and 4(f), which represent low and high temperatures, respectively. Here, the top panels show the band structure and the bottom ones show the Fermi surfaces. The blue/redshifts in FeSe tend to decrease with increasing temperature, thus resulting in a simultaneous growth of all Fermi surfaces.

Variations of the electronic structure with temperature have been detected earlier and in different materials. For instance, charge density wave bearing $TaSe_2$ exhibits a pronounced T-dependent Fermi surface shape and its nesting. This behavior was attributed to the presence of a pseudogap, nonmonotonically varying with temperature [31,32]. Also, in

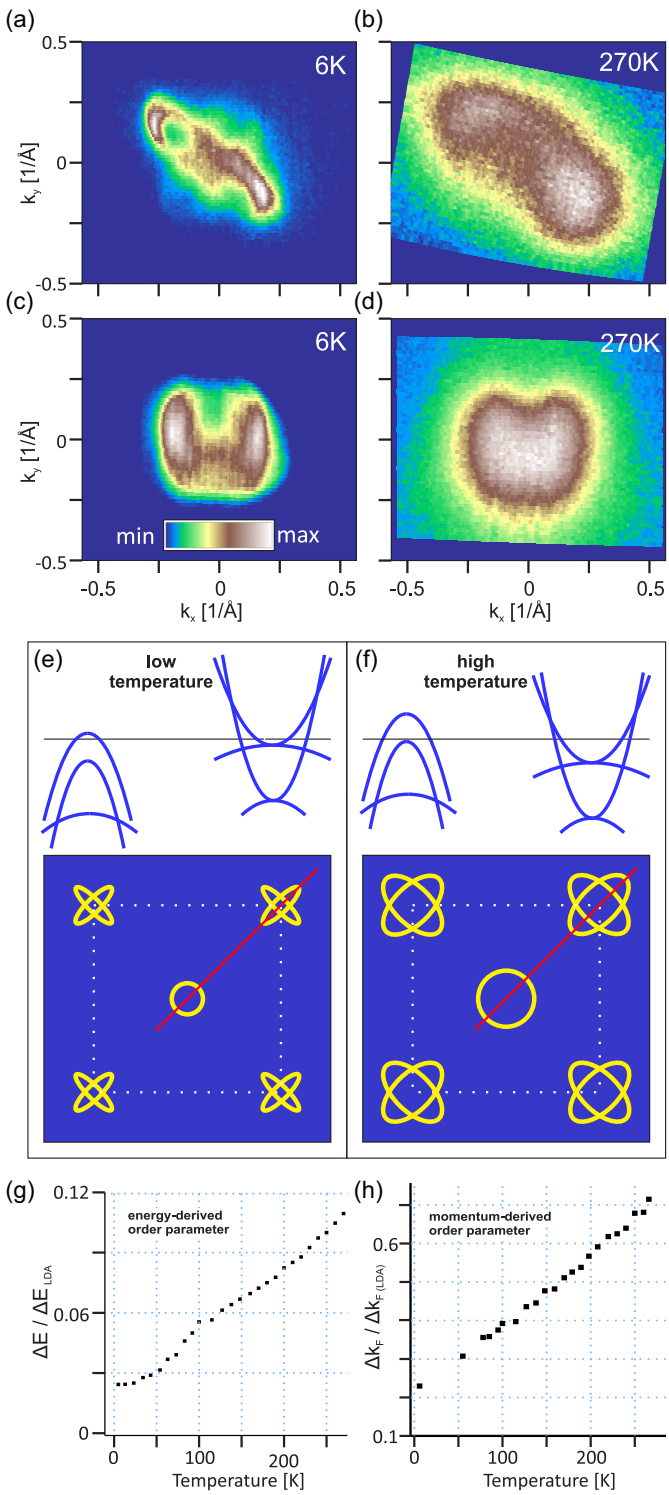

FIG. 4. (a), (c) Fermi surface maps measured at 6 K near the corner and the center of the BZ, respectively. (b), (d) Similar maps measured at 270 K. Sketches in (e) and (f) represent the band structure and Fermi surface at low and high temperatures, respectively. (g) Energy distance between the top of the middle hole band and the bottoms of the electron pockets [see (e) and (f)] normalized to the calculated value. (h) Momentum width of the electron pocket normalized to the calculated value.

IBSs, the temperature dependence was found in undoped and electron-doped 122 materials [10,33]. Both studies reported

the shrinking of the hole pocket and expansion of the electron one and thus a considerable increase of charge carrier density upon warming up the samples. This is in contrast to our observations in FeSe, where both Fermi surfaces expand with temperature. Interestingly, the Fermi surface of a hole-doped 122 material taken at room temperature did not show any noticeable departure from the low-temperature version [8]. We point out that the electronic structure of FeSe is simpler than that of 122 compounds because it is tetragonal at higher temperatures, does not undergo folding due to the spin density wave (SDW) phase at low temperatures, and is less three dimensional. Therefore, the temperature-dependent variations should be seen more clearly in FeSe.

Two theoretical approaches seem to explain the blue/redshifts in IBSs at low temperatures. The first one is the electronic instability called the Pomeranchuk effect [13,15,16,18,19]. Forward scattering triggers a distortion of the Fermi surface which preserves the point group symmetry of the crystal. The area of both the electron and hole pockets increases (or decreases) so that the total charge density remains constant [13,15]. The second approach is based on the renormalization of the bands by spin fluctuations via self-energy effects [12,14]. The blue/redshifts and shrinking of the FS reported by ARPES are considered as a direct consequence of the coupling to a bosonic mode upon a proper accounting of particle-hole asymmetry and the multiband character. It has been also suggested [28] that the blue/redshifts can be understood as a suppression of nearest-neighbor hopping due to spin/orbital orderings.

In the present study we report on the temperature dependence of the electronic structure, which may help to distinguish between these two theoretical approaches. The S_{+-} Pomeranchuk effect will result in a mean-field order parameter which is the relative shift of the electron bands in the corners and hole bands in the center of the BZ. As any mean-field order parameter, it will diminish as temperature increases and will disappear at a particular critical temperature. In the case of spin-fluctuation-induced shifts, the latter will decrease with temperature as well, but this behavior will be dictated by the softening of the spin-fluctuation spectrum and therefore will evolve more smoothly.

In Figs. 4(g) and 4(h) we present two quantities which can be considered as the energy- and momentum-derived order parameters of the phenomenon. Figure 4(g) shows a temperature evolution of the energy separation between the top of the middle hole band and the value which we use for characterization of the EDC from near the corner of the BZ [Fig. 3(e)]. This parameter is given in units of a fraction of this distance to the one obtained in LDA calculations [2]. To estimate this parameter for low temperatures, we used the mean values of the energy positions of all four peaks extracted from the EDC measured at 6 K. The monotonic and slightly superlinear increase with a signature of the nematic transition reflects the experimental observations discussed above. The second parameter [Fig. 4(h)] is obtained by relating the momentum width of the electron pocket [Figs. 4(a) and 4(b)] to the width obtained in band structure calculations. Here, the temperature dependence only slightly deviates from linear above 200 K without any pronounced signatures related to the nematic transition.

The behavior of both parameters does not seem to be in immediate agreement with either of the theoretical approaches mentioned above. If the curve from Fig. 4(g) does resemble the behavior of the typical mean-field order parameter expected in the case of the S_{+-} Pomeranchuk effect, the momentum-related quantity does not. The observed quasilinear behavior is most likely not expected also when considering coupling to spin fluctuations. The most striking result is that in spite of rather high temperatures, both parameters still indicate a considerable departure from LDA, implying either an extremely high onset temperature of the Pomeranchuk instability or a very unusual temperature decay of the spin-fluctuation spectrum. In any case, our results call for a more thorough theoretical investigation aiming at a quantitative explanation of the temperature relaxation.

In conclusion, in this Rapid Communication, we demonstrated that the band structure near the corner and the center of the BZ monotonically changes with temperature from 6 K to room temperature. This change reduces the size of the blue/redshifts and expands both parts of the Fermi surface. Both parameters characterizing the effect in terms of energy and momentum are hard to reconcile with existing theoretical approaches.

We are grateful to R. Fernandes, A. Chubukov, D.-H. Lee, L. Benfatto, L. Fanfarillo, and A. Yaresko for fruitful discussions. We thank Diamond Light Source for access to beamline I05 (Proposal No. si11543-1), and T. Kim and M. Hoesch for the help at the beamline. The work is supported by Deutsche Forschungsgemeinschaft Grants No. BO1912/6-1 and No. BO1912/7-1.

[1] J. Maletz, V. Zabolotnyy, D. Evtushinsky, S. Thirupathaiah, A. Wolter, L. Harnagea, A. Yaresko, A. Vasiliev, D. Chareev, A. Böhmer *et al.*, Phys. Rev. B **89**, 220506 (2014).

[2] A. Fedorov, A. Yaresko, T. K. Kim, Y. Kushnirenko, E. Haubold, T. Wolf, M. Hoesch, A. Grüneis, B. Büchner, and S. V. Borisenko, Sci. Rep. **6**, 36834 (2016).

[3] A. A. Kordyuk, V. B. Zabolotnyy, D. V. Evtushinsky, A. Yaresko, B. Büchner, and S. V. Borisenko, J. Supercond. Novel Magn. **26**, 2837 (2013).

[4] D. V. Evtushinsky, A. N. Yaresko, V. B. Zabolotnyy, J. Maletz, T. K. Kim, A. A. Kordyuk, M. S. Viazovska, M. Roslova, I. Morozov, R. Beck *et al.*, Phys. Rev. B **96**, 060501(R) (2017).

[5] G. Kotliar, S. Y. Savrasov, K. Haule, V. S. Oudovenko, O. Parcollet, and C. A. Marianetti, Rev. Mod. Phys. **78**, 865 (2006).

[6] M. Aichhorn, S. Biermann, T. Miyake, A. Georges, and M. Imada, Phys. Rev. B **82**, 064504 (2010).

[7] J. Ferber, K. Foyevtsova, R. Valentí, and H. O. Jeschke, Phys. Rev. B **85**, 094505 (2012).

[8] V. B. Zabolotnyy, D. S. Inosov, D. V. Evtushinsky, A. Koitzsch, A. A. Kordyuk, G. L. Sun, J. T. Park, D. Haug, V. Hinkov, A. Boris *et al.*, Nature (London) **457**, 569 (2009).

[9] S. V. Borisenko, D. V. Evtushinsky, Z.-H. Liu, I. Morozov, R. Kappenberger, S. Wurmehl, B. Büchner, A. N. Yaresko, T. K. Kim, M. Hoesch *et al.*, Nat. Phys. **12**, 311 (2016).

[10] V. Brouet, P.-H. Lin, Y. Texier, J. Bobroff, A. Taleb-Ibrahimi, P. Le Fèvre, F. Bertran, M. Casula, P. Werner, S. Biermann *et al.*, Phys. Rev. Lett. **110**, 167002 (2013).
[11] S. V. Borisenko, Nat. Mater. **12**, 600 (2013).
[12] L. Ortenzi, E. Cappelluti, L. Benfatto, and L. Pietronero, Phys. Rev. Lett. **103**, 046404 (2009).
[13] H. Zhai, F. Wang, and D.-H. Lee, Phys. Rev. B **80**, 064517 (2009).
[14] L. Benfatto and E. Cappelluti, Phys. Rev. B **83**, 104516 (2011).
[15] J. C. S. Davis and D.-H. Lee, Proc. Natl. Acad. Sci. USA **110**, 17623 (2013).
[16] A. V. Chubukov, M. Khodas, and R. M. Fernandes, Phys. Rev. X **6**, 041045 (2016).
[17] L. Fanfarillo, J. Mansart, P. Toulemonde, H. Cercellier, P. Le Fèvre, F. Bertran, B. Valenzuela, L. Benfatto, and V. Brouet, Phys. Rev. B **94**, 155138 (2016).
[18] R.-Q. Xing, L. Classen, M. Khodas, and A. V. Chubukov, Phys. Rev. B **95**, 085108 (2017).
[19] L. Classen, R.-Q. Xing, M. Khodas, and A. V. Chubukov, Phys. Rev. Lett. **118**, 037001 (2017).
[20] M. Hoesch, T. K. Kim, P. Dudin, H. Wang, S. Scott, P. Harris, S. Patel, M. Matthews, D. Hawkins, S. G. Alcock *et al.*, Rev. Sci. Instrum. **88**, 013106 (2017).
[21] M. D. Watson, T. K. Kim, A. A. Haghighirad, N. Davies, A. McCollam, A. Narayanan, S. F. Blake, Y. L. Chen, S. Ghannadzadeh, A. J. Schofield *et al.*, Phys. Rev. B **91**, 155106 (2015).
[22] K. Nakayama, Y. Miyata, G. N. Phan, T. Sato, Y. Tanabe, T. Urata, K. Tanigaki, and T. Takahashi, Phys. Rev. Lett. **113**, 237001 (2014).
[23] P. Zhang, T. Qian, P. Richard, X. Wang, H. Miao, B. Lv, B. Fu, T. Wolf, C. Meingast, X. Wu *et al.*, Phys. Rev. B **91**, 214503 (2015).
[24] H. C. Xu, X. H. Niu, D. F. Xu, J. Jiang, Q. Yao, Q. Chen, Q. Song, M. Abdel-Hafiez, D. Chareev, A. Vasiliev *et al.*, Phys. Rev. Lett. **117**, 157003 (2016).
[25] T. Shimojima, Y. Suzuki, T. Sonobe, A. Nakamura, M. Sakano, J. Omachi, K. Yoshioka, M. Kuwata-Gonokami, K. Ono, H. Kumigashira *et al.*, Phys. Rev. B **90**, 121111 (2014).
[26] Z. R. Ye, C. F. Zhang, H. Ning, W. Li, L. Chen, T. Jia, M. Hashimoto, D. H. Lu, Z.-X. Shen, and Y. Zhang, arXiv:1512.02526.
[27] M. D. Watson, T. K. Kim, L. C. Rhodes, M. Eschrig, M. Hoesch, A. A. Haghighirad, and A. I. Coldea, Phys. Rev. B **94**, 201107(R) (2016).
[28] Y. V. Pustovit and A. A. Kordyuk, Low Temp. Phys. **42**, 995 (2016).
[29] The crossed ellipses themselves are not from different domains, unlike the pockets in the center. Their presence is already expected in the tetragonal phase. Nematicity influences this portion of the FS in a less pronounced manner (see Ref. [2]). Also, the ellipses in the corners do not actually cross each other because of a spin-orbit interaction. There is one small and one big electron pocket which only resemble crossed ellipses.
[30] See Supplemental Material at http://link.aps.org/supplemental/10.1103/PhysRevB.96.100504 for the discussion of fitting procedure.
[31] S. V. Borisenko, A. A. Kordyuk, A. N. Yaresko, V. B. Zabolotnyy, D. S. Inosov, R. Schuster, B. Büchner, R. Weber, R. Follath, L. Patthey *et al.*, Phys. Rev. Lett. **100**, 196402 (2008).
[32] D. S. Inosov, D. V. Evtushinsky, V. B. Zabolotnyy, A. A. Kordyuk, B. Büchner, R. Follath, H. Berger, and S. V. Borisenko, Phys. Rev. B **79**, 125112 (2009).
[33] R. S. Dhaka, S. E. Hahn, E. Razzoli, R. Jiang, M. Shi, B. N. Harmon, A. Thaler, S. L. Bud'ko, P. C. Canfield, and A. Kaminski, Phys. Rev. Lett. **110**, 067002 (2013).